IMPACT OF COLD SURGE (CS) ON NET SURFACE HEAT FLUX (NSHF) IN NATUNA SEA

Rezfiko Agdialta[1,4]*, Nining Sari Ningsih[2], Nurjanna Joko Trilaksono[3]
[1]Indonesian Agency for Meteorological, Climatological and Geophysics (BMKG).
[2]Environmental and Applied Oceanography Research Group, Faculty of Earth Sciences and Technology, Bandung Institute of Technology (ITB).
[3]Atmospheric Science Research Group, Faculty of Earth Sciences and Technology, Bandung Institute of Technology (ITB).
[4]Master's Program in Earth Sciences, Faculty of Earth Sciences and Technology, Bandung Institute of Technology (ITB).
**E-mail: rezfikoagdialta@gmail.com*

Article submitted: August 16, 2024 Article revised: October 21, 2024 Article accepted: November 5, 2024

ABSTRACT

Cold Surge (CS) events are often associated with rainfall occurrences in the Jakarta area. However, there is still limited literature on how CS affects other parameters in Indonesia. This study aims to contribute to this literature, particularly regarding the crucial role of CS in the interaction between the ocean and the atmosphere. This research uses the composite difference method to compare changes in Wind Speed (WS), Latent Heat Flux (LHF), Sensible Heat Flux (SHF), Shortwave Radiation (SWR), Longwave Radiation (LWR), and Net Surface Heat Flux (NSHF) during CS phases versus neutral conditions no CS (nCS). The composite difference results indicate an increase in wind speed in the study area, Natuna Sea, with values of 1.17 m/s, 1.45 m/s, and 1.69 m/s for December, January, and February, respectively. This finding explains that the increase in wind speed significantly influences LHF in the negative direction, meaning more LHF is transferred from the ocean to the atmosphere during the CS phase. LHF also predominantly affects NSHF in the study area during the CS period, indicating that more NSHF is leaving the ocean and entering the atmosphere compared to the amount entering the ocean from the atmosphere during the CS phase.

Keywords: Cold Surge, Latent Heat Flux, Shortwave Radiation, Wind Speed

1. Introduction

Cold Surge (CS) is a phenomenon that frequently occurs in East Asia and Southeast Asia during the boreal winter [1]. CS can cause an increase in mean sea level pressure (MSLP), which in turn leads to an increase in wind speed [2, 3]. CS can lead to drops in air temperature and increased precipitation in many locations [4]. In the process, winds from the Northern Hemisphere carry cold air from the Arctic region to East Asia, which can cause a rapid drop in temperature in the areas they pass through [5]. CS is related to the spread of cold air masses originating from the Siberian region, which then move into Mongolia and can extend as far as northern China [6]. Siberian High (SH) is a significant anticyclone activity that plays a crucial role in the distribution of cold air from the Northern Hemisphere to East Asia during Boreal Winter, the winter season in the Northern Hemisphere [7]. The occurrence of strong CS is closely related to the intensity of SH, meaning that SH events associated with the increased mean sea level pressure over Siberia are the primary factor causing CS [8].

The latest approach for analyzing the onset of cold surges (CS) involves examining the Mean Sea Level Pressure (MSLP) in the region of 18°N–22°N and 105°E–122°E, which must be above 1020 hPa, as well as the average wind speed in the area of 5°N–10°N and 107°E–115°E, which must exceed 9.65 m/s [9]. Cold surges can also extend to Southeast Asia and trigger numerous convective activities [10]. A CS that extends across the equator in western Indonesia is known as the Cross-Equatorial Northerly Surge (CENS) [11]. CENS was first introduced by Hattori et al. (2011) [12], characterized by an increase in the average meridional wind speed in the region of 105°E to 115°E to more than 5 m/s. CS and CENS events are often associated with increased precipitation and a higher frequency of rainfall events, which can lead to flooding [13, 14, 15].

CENS originates from the southward spread of CS. Rainfall in Jakarta associated with CENS can occur due to moisture transport from the South China Sea to Jakarta. This rainfall is linked to the formation of high convective clouds and results in an increased frequency of rainfall events in Jakarta [16]. Rainfall events in the North Coast of West Java also associated with CENS, particularly those occurring during the

Early Morning (EM) phase, typically between 01:00 and 04:00 WIB (Waktu Indonesia Barat: Western Indonesia Time is UTC +7 hours). EM phase rainfall may be due to the increased frequency of convective cloud movement from the sea to the land in the North Coast of West Java during this period [17].

CS and CENS events are associated with increases in wind speed. This increase in wind speed can affect changes in latent heat flux (LHF). LHF can influence Net Surface Heat Flux (NSHF). Wind speed variability and the difference in specific humidity between the near-surface ocean layer and the atmosphere play a major role in influencing SST [18]. Based on the analysis of wind speed and the difference in specific humidity between the near-surface ocean and the atmosphere, it can be concluded that during an increase in SST, there is a significant decrease in wind speed, which is followed by a reduction in LHF from the ocean to the atmosphere [19]. In tropical regions globally, changes in wind speed can affect SST. As wind speed increases, the transfer of LHF from the ocean to the atmosphere also increases, indicating that the ocean is losing latent heat. This change in LHF can influence NHF, which in turn can affect the rate of change of SST over time [20].

The decrease in SST in the Java Sea is influenced by the release of LHF from the ocean to the atmosphere. The release of LHF from the ocean to the atmosphere in the Java Sea will increase with increasing wind speed. Conversely, the lower the wind speed in the Java Sea, the LHF from the ocean to the atmosphere will also decrease, causing a decrease in heat release and can increase SST [21]. This study analyzes the impact of cold surge (CS) events closely associated with increased wind speed. The research will investigate how changes in wind speed resulting from CS events can influence latent heat flux (LHF), sensible heat flux (SHF), and net surface heat flux (NSHF) in the Natuna Sea. This study seeks to examine the extent to which the parameters of heat exchange between the ocean and the atmosphere in the research area are affected by variations in wind speed. Additionally, it aims to serve as a reference for further studies in understanding the long-term impacts of CS on changes in SST.

2. Methods

The study area is located in the Natuna Sea, geographically situated between 105°-110°E and 2.5°N-5°N. The study area is marked with a red line in Figure 1. The reason for selecting this area is that it is the northernmost part of Indonesia, making it the region with the most significant influence on cold surge (CS) events.

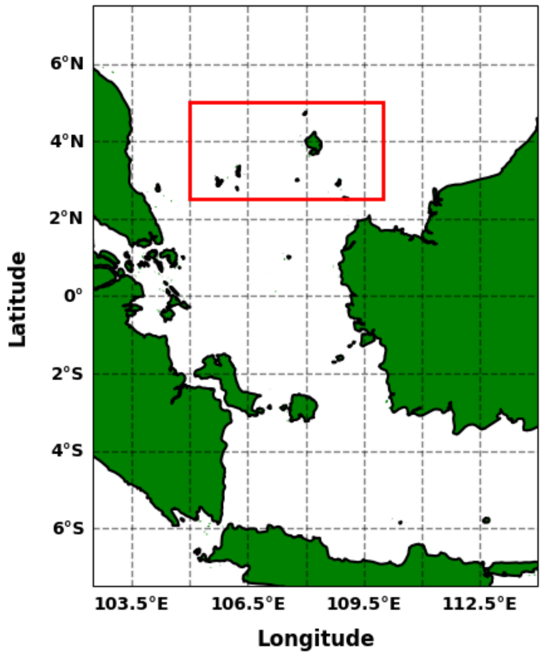

Figure 1. The study area is marked by a red box outline

The parameters to be analyzed in this study are Wind Speed (WS), Latent Heat Flux (LHF), Sensible Heat Flux (SHF), Shortwave Radiation (SWR), Longwave Radiation (LWR), and Net Surface Heat Flux (NSHF) during cold surge (CS) events.

The data used in this study are reanalysis data from ERA5 with a spatial resolution of 0.25° x 0.25°, or approximately 27.7 km x 27.7 km. This data includes wind speed at 850 mb, MSLP, surface wind speed, LHF, SHF, SWR, LWR, and SST. The reason for choosing ERA5 reanalysis data is that reanalysis data are an improved type of data derived from existing datasets, providing more representative results of actual environmental conditions.

Removing Data Related to ENSO, IOD, and MJO. The first step in this study is to filter the data for the phases of ENSO (El Niño Southern Oscillation), IOD (Indian Ocean Dipole), and MJO (Madden-Julian Oscillation) (Phases 3, 4, and 5) from 2000 to 2023 to better understand the impact of cold surges (CS). Ultimately, the dates selected for further analysis include only those when CS events occurred without any other coinciding events.

El Niño is characterized by an increase in SST in the Niño 3.4 zone with an anomaly value greater than 0.5 °C for five consecutive months. Conversely, La Niña is the opposite of El Niño, occurring when the SST anomaly in the Niño 3.4 zone is less than -0.5 °C for five consecutive months [22, 23].

In contrast, the IOD can be identified based on the SST anomaly values in the eastern and western regions of the Indian Ocean. A Dipole Mode Index

(DMI) anomaly value greater than 0.4°C indicates a positive IOD condition, while an SST anomaly value less than -0.4°C indicates a negative IOD [24].

The propagation of oscillatory waves moving eastward with a duration of about 30 to 90 days is known as the MJO [25]. MJO is one of the most dominant oscillations occurring in tropical regions [26].

Detection of CS. Following Lim et al. (2017) [9], we identify CS events based on MSLP and average wind speed. CS can be considered if the MSLP value at D2 (18°N–22°N and 105°E–122°E), is greater than 1020 hPa at H-2 or H-1 (H-2 refers to two days before the CS event, while H-1 refers to one day before the CS event). Beside MSLP value, an average wind speed at D1 (5°N–10°N and 107°E–115°E), should be greater than 9.65 m/s at H-1 or H (H refers to the day during the CS event). If the both condition (MSLP and wind speed) is satisfied, then it can be categorized as a CS.

Wind Speed Evaluation. The wind speed calculation is performed using the zonal wind component (u) and the meridional wind component (v), which are then combined to compute the magnitude of the wind speed using the following equation:

$$V = \sqrt{u^2 + v^2} \tag{1}$$

From equation (1), u is the zonal wind component in m/s, v is the meridional wind component in m/s, and V is the magnitude of the wind speed in m/s.

NSHF Evaluation. NSHF is a key parameter in the process of sea-atmosphere interactions in Indonesian waters. A positive value indicates a net transfer of heat from the atmosphere to the sea, while a negative value indicates that the sea is losing heat to the atmosphere [27]. NSHF is the total heat exchange between the sea and the atmosphere, derived from the sum of SWR, LWR, SHF, and LHF. NSHF can influence both meteorological and oceanographic processes occurring in the sea and the atmosphere [28]. To calculate the Net Surface Heat Flux (NSHF), the following equation can be used:

$$Q_{NSHF} = Q_{SWR} + Q_{LWR} + Q_{SHF} + Q_{LHF} \tag{2}$$

Q_{SWR} is shortwave radiation (W/m²), Q_{LWR} is longwave radiation flux (W/m²), Q_{SHF} is sensible heat flux (W/m²), Q_{LHF} is latent heat flux (W/m²), and Q_{NSHF} is net surface heat flux (W/m²). Shortwave radiation is the radiation derived from solar energy, consisting of incoming radiation and radiation reflected back to the atmosphere [29]. The equation used for calculating shortwave radiation is as follows:

$$Q_{SWR} = S \cdot (1 - \alpha) \tag{3}$$

S is the solar radiation reaching the Earth's surface before any is reflected back to the atmosphere (W/m²), α is the albedo that reflects radiation back to the atmosphere from the Earth's surface, and Q_{SWR} is the shortwave radiation (W/m²). Longwave radiation is the thermal radiation emitted from the land surface or the sea surface to the atmosphere. Longwave radiation is related to the surface temperature of the land or sea. The higher the temperature of an object emitting longwave radiation, the greater the intensity of the longwave radiation [30]. The equation used to calculate the intensity of longwave radiation is as follows:

$$Q_{LWR} = 0.97 \cdot (5.67 \cdot 10^{-8}) \cdot (SST + 273.15)^4 - L \tag{4}$$

Equation (4) relates to the Stefan-Boltzmann Law, which states that the intensity of radiation depends on the surface temperature of the object emitting the radiation [31]. $5.67 \cdot 10^{-8}$ is Stefan-Boltzmann constant, SST is Sea Surface Temperature (°C), 273.15 is conversion factor from Celsius to Kelvin, L is the thermal radiation emitted by the earth surface or the ocean surface (W/m²), and Q_{LWR} is longwave radiation (W/m²).

Sensible heat flux is the transfer of heat between the ocean and the atmosphere without any accompanying phase changes in the substance. The equation used to calculate sensible heat flux can be written as follows:

$$Q_{SHF} = \rho C_p C_s (U_a - U_s)(T_s - T_a) \tag{5}$$

where ρ is the air density (kg/m³), C_p is heat capacity of air (J/Kg K), $U_a - U_s$ is the difference in wind speed between the surface layer and the layer close to the sea surface (m/s), $T_s - T_a$ is the difference in temperature between the surface layer and the layer close to the sea surface (°C), and Q_{SHF} is sensible heat flux (W/m²). Latent Heat Flux can be defined as the transfer of latent heat between the Earth's surface or the ocean surface and the atmosphere, associated with the processes of water evaporation at the surface and condensation of water vapor in the troposphere. Latent Heat Flux reflects the phase change of a substance from liquid (water) to gas (water vapor) and vice versa [32]. The equation used to calculate LHF can be expressed as follows:

$$Q_{LHF} = pLC_L (U_a - U_s)(Q_s - Q_a) \tag{6}$$

where ρ is the air density (kg/m³), L is the latent heat of water vapor (2.25×10^6 J/kg), $U_a - U_s$ is the difference in wind speed between the surface layer (10-m) and the ocean near-surface layer (m/s), and $Q_s - Q_a$ is the difference in specific humidity between the surface layer and the layer close to the sea surface (kg/kg), and Q_{LHF} is latent heat flux (W/m²).

LHF is explained by the differences between $U_a - U_s$ and $Q_s - Q_a$, which demonstrate how wind speed and specific humidity can influence LHF. Since LHF is related to the evaporation process, wind speed plays a crucial role. An increase in wind speed over the ocean surface facilitates evaporation. Therefore, a negative value of $U_a - U_s$ indicates a higher wind speed near the ocean surface, which supports the evaporation process and thus influences LHF, and vice versa.

The value of $Q_s - Q_a$ represents the difference in specific humidity between the layer near the ocean surface and the layer above it. The positive value of $Q_s - Q_a$ indicates that the layer above the ocean surface has a higher specific humidity. This condition also supports the evaporation process because the water vapor content in the atmospheric layer has not yet reached saturation, resulting in increased evaporation, which is related to LHF.

Composite Difference. The composite difference method is used to compare two different datasets. This method involves calculating the difference between the composite data during nCS (no CS) phase and the composite data during the CS phase. It is utilized to assess how the variability parameters such as WS, LHF, SHF, SWR, LWR, and NSHF relative to their neutral conditions.

3. Result and Discussion

Table 1 shows the results of filtering ENSO, IOD, and MJO (Phases 3, 4, 5) from the year 2000 to 2023 for the months of December, January, and February. Based on Table 1, it can be concluded that there are 13 neutral periods, with 3 periods in December, 4 periods in January, and 6 periods in February.

Figure 2 shows the MSLP on (a) December 26, 2001, (b) December 27, 2001, (c) December 28, 2001, (d) December 29, 2001, (e) December 30, 2001, and (f) December 31, 2001. On all these dates, the MSLP values in the D2 region (18°N–22°N and 105°E–122°E), indicated by the red outline boxes, are greater than 1020 hPa, indicating high-pressure conditions in that area. Since wind moves from high pressure to low pressure, the high pressure in this region leads to an increase in wind speed in the D1 region (5°N–10°N and 107°E–115°E), as shown in Figure 3, where the average wind speed must exceed 9.65 m/s at H-1 or H. From Figure 3, it can be seen that wind speeds greater than 9.65 m/s occurred on December 28, 2001, with an average wind speed of 11.11 m/s. Therefore, it can be concluded that the CS period began on December 28, 2001 and weaken on December 31, 2001, with an average wind speed anomaly in the D1 region of 6.72 m/s. The grouping of CS and nCS event dates is shown in Table 2 and Table 3.

Table 2 shows the number of CS events during neutral periods. In the neutral periods, there were 6 CS events in December, 7 CS events in January, and 5 CS event in February.This result is consistent with the previous study that showed that CS events are more frequent in January than in December [33]. However, there is a slight difference in approach in this study, as all CS events are considered without considering other phenomena such as the Cross-Equatorial Northerly Surge (CENS).

Meanwhile, Table 3 shows the number of nCS events during neutral periods. In the neutral periods, there were 6 nCS events in December, 8 nCS events in January, and 9 nCS events in February. The values on the CS and nCS events will be composited for each phase and further analyzed using the composite difference method. Tabel 3 shows the anomalies of parameters such as WS, LHF, SHF, SWR, LWR, and NSHF during the CS phase compare to those during the nCS (neutral) phase.

Table 1. Neutral Periods Without ENSO, IOD, and MJO (Phases 3, 4, and 5) during December, January, and February

No	Neutral Periods		
	December	**January**	**February**
1	December 8–31, 2001	January 1–20, 2002	February 21–28, 2002
2	December 1–6, 2003	January 1–27, 2004	February 12–25, 2004
3	December 23–31, 2003	January 11–13, 2013	February 1–14, 2013
4		January 3–11, 2014	February 25–28, 2013
5			February 1–5, 2014
6			February 13–28, 2014

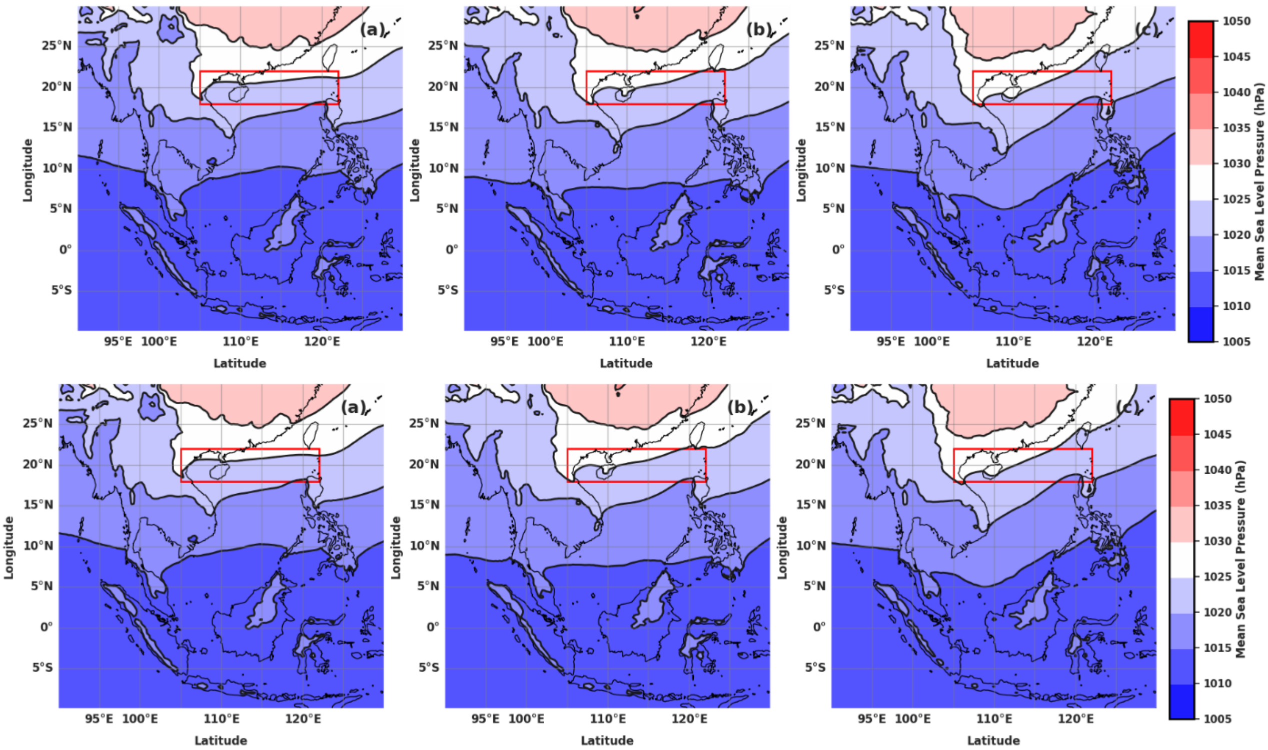

Figure 2 Mean Sea Level Pressure on (a) December 26, 2001, (b) December 27, 2001, (c) December 28, 2001, (d) December 29, 2001, (e) December 30, 2001, and (f) December 31, 2001

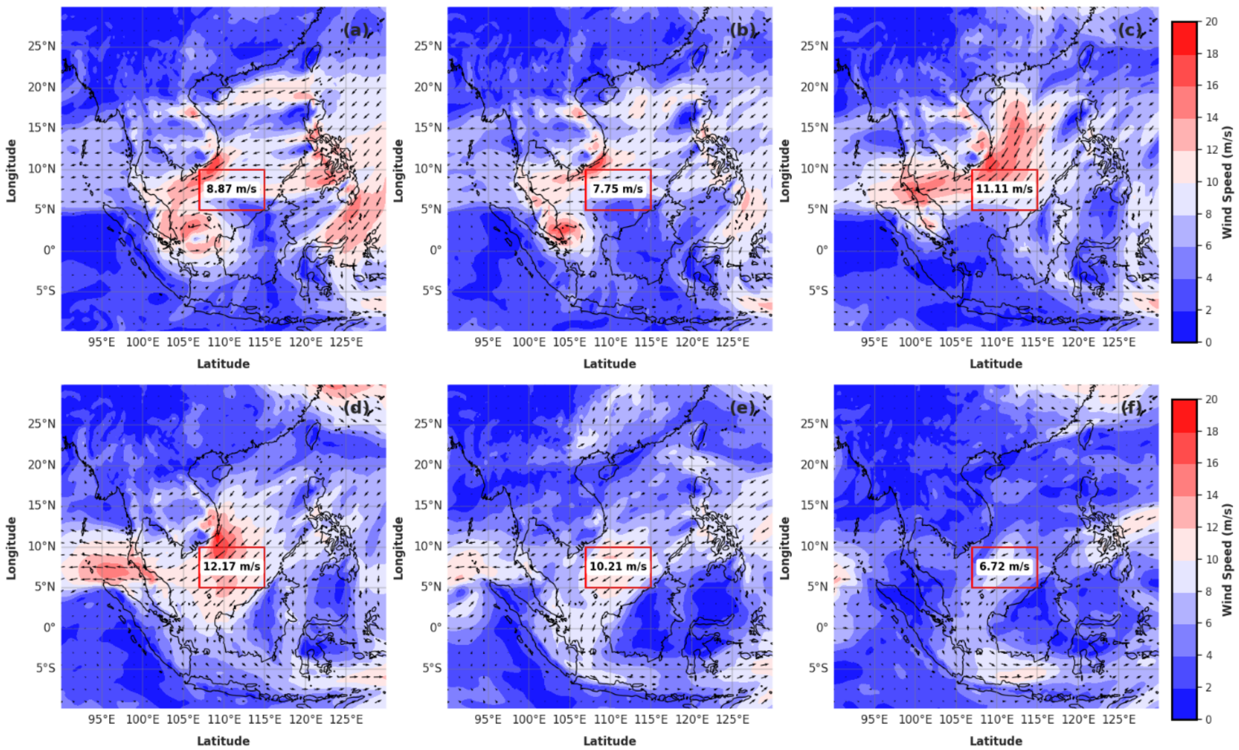

Figure 3 Same as Figure 2 but for wind speed at the 850 hPa level

Table 2. Dates of CS events

No	December	January	February
1	December 8, 2001	January 3–9, 2002	February 12–13, 2004
2	December 11–12, 2001	January 20, 2002	February 1–3, 2013
3	December 19–20, 2001	January 11, 2013	February 9–14, 2013
4	December 28–31, 2001	January 8, 2004	February 21–23, 2013
5	December 23, 2003	January 21–27, 2004	February 25, 2013
6	December 27–31, 2003	January 5–6, 2014	
7		January 9, 2014	

Table 3. Same as Table 2 but for nCS events

No	December	January	February
1	December 9–10, 2001	January 1–3, 2002	February 22–28, 2002
2	December 13–17, 2001	January 10–14, 2002	February 14–21, 2003
3	December 18, 2001	January 15–19, 2002	February 14–25, 2004
4	December 21–27, 2001	January 1–2, 2004	February 4–8, 2013
5	December 1–6, 2003	January 5–7, 2004	February 26–28, 2013
6	December 24–26, 2003	January 10–20, 2004	February 3–4, 2014
7		January 12–23, 2013	February 7–8, 2014
8		January 10–11, 2014	February 13–20, 2014
9			February 24–28, 2014

The composite difference method is used to examine how CS events deviate from nCS conditions. Figure 4 shows the composite difference between CS and nCS events. During the CS period, the average wind speed in the study area increased by 1.17 m/s in December, 1.45 m/s in January, and 1.69 m/s in February. This increase in wind speed is accompanied by latent heat flux (LHF) shifting from the ocean to the atmosphere, as shown in Table 4, with a correlation value of -0.66. The correlation calculated by averaged spatial correlation in the research area. It indicates that an increase in wind speed will cause an increase in LHF in the negative direction, from the ocean to the atmosphere. This result is consistent with the research conducted by Zhang and Rossow (1997) [34] that wind speed is an important factor influencing LHF during the winter season in the Indo-Western Pacific region.

In the tropics, shortwave radiation from the sun is the dominant energy input received by the land or sea surface. While latent heat flux is the dominant energy output that influences net surface heat flux in the region [35]. The research by Tomita and Kubota, (2004) [36] explains that latent heat flux and shortwave radiation predominantly contribute to influencing net surface heat flux in an area located in Indonesia where its climate variability is influenced by monsoon patterns. However, this study shows that an increase in wind speed can enhance latent heat flux in a negative direction, ultimately making the contribution of latent heat flux more dominant than that of shortwave radiation to net surface heat flux. As shown in Table 4, the anomaly of shortwave radiation in the study area during the CS phase tends to be negative. It indicates that less heat is absorbed by the ocean from sunlight during this period. The SWR anomaly observed during January and February presents negative values, indicating reduced solar radiation reaching the ocean surface, caused by cloud cover.

The research by Feng et al. (2016) [37] also states that LHF component is the most dominant factor influencing NSHF in the South China Sea. This finding is consistent with the correlation value of 0.94 between LHF and NSHF in the Natuna Sea. It indicates a strong relationship between NSHF and LHF, meaning that LHF predominantly influences NSHF. The average anomaly value of NSHF for December, January, and February is -25.26 W/m², indicating that more heat is being transferred from the ocean to the atmosphere, influenced by LHF, during the CS period. Meanwhile, the average anomaly values for SHF and LWR are relatively low in December, January, and February, as shown in Table 4. These values indicate that SHF and LWR anomalies have a minor impact on changes in NSHF.

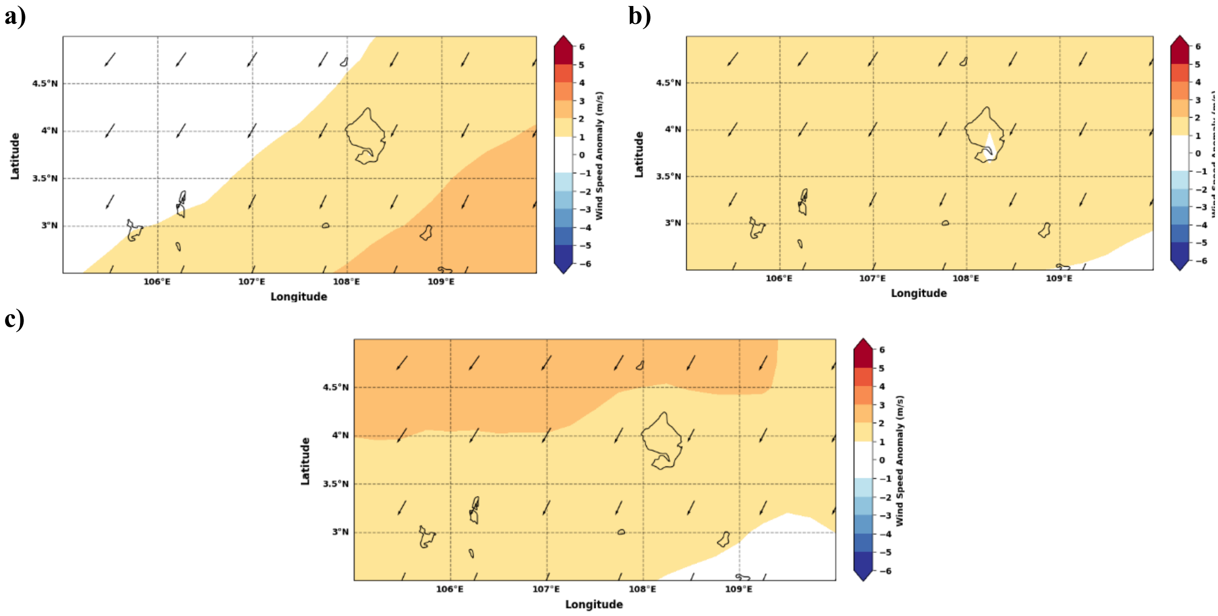

Figure 4. Composite difference (CS and nCS) for surface wind speed (a) December, (b) January, and (c) February

Table 4. Average composite difference values for WS, LHF, SHF, SWR, LWR, and NSHF parameters in the study area.

Month	WS (m/s)	LHF (W/m^2)	SHF (W/m^2)	SWR (W/m^2)	LWR (W/m^2)	NSHF (W/m^2)
December	1.17	-10.20	2.66	54.42	-8.08	38.80
January	1.45	-20.63	-3.18	-41.37	5.89	-59.29
February	1.69	-16.81	-3.39	-44.74	9.64	-55.30

4. Conclusion

NSHF plays a crucial role in heat energy exchange between the ocean and the atmosphere. This study explains that during the CS period, there is an increase in wind speed in the study area. This increase in wind speed is significant in enhancing latent heat flux from the ocean to the atmosphere. The correlation between wind speed and latent heat flux is -0.66, indicating a strong relationship. LHF also predominantly affects latent heat flux, with a correlation value of 0.94. Latent heat flux largely influences the net heat exchange between the ocean and the atmosphere. Therefore, wind speed plays a role in enhancing latent heat flux during the CS phase, affecting the net heat flux between the ocean and the atmosphere. SWR during cold surge (CS) events in January and February exhibits negative values typically associated with cloud cover. Negative SWR values indicate a reduction in shortwave radiation reaching the Earth's surface, suggesting an increase in cloud cover over the region. Future studies should aim to elucidate the effects of CS events in relation to cloud cover and examine their influence on variations in both shortwave and longwave radiation, as this research area still needs to be explored.

References

[1] I. Tan, M. J. Reeder, M. S. Singh, C. E. Birch, and S. C. Peatman, "Wet and dry cold surges over the Maritime Continent," *Journal of Geophysical Research: Atmospheres*, vol. 128, p. e2022JD038196, 2023. [Online]. Available: https://doi.org/10.1029/2022JD038196.

[2] M.-L. Chong, H.-Y. Yeung, and K.-K. Hon, "Study of extreme cold surge in Hong Kong," *Meteorology*, vol. 2, no. 1, pp. 52-71, 2023, doi: 10.3390/meteorology2010004. [Online]. Available:https://doi.org/10.3390/meteorology2010004.

[3] J. Lin and H.-N. Cheung, "Distinct mid-latitude Eurasian Rossby wave trains preceding strong and weak cold surges in Southern China," *Frontiers in Earth Science*, vol. 10, 2022, doi: 10.3389/feart.2022.861015. [Online]. Available:https://doi.org/10.3389/feart.2022.861015.

[4] H. G. Takahashi, "Orographic low-level clouds of Southeast Asia during the cold surges of the winter monsoon," *Atmospheric Research*, vol. 131, pp. 22–33, 2013, doi: 10.1016/j.atmosres.2012.07.00.
[5] A. Kumar, "A new approach to cold surge classification in East Asia," *Scientific Reports*, vol. 11, p. 23659, 2021. [Online]. Available: https://doi.org/10.1038/s41598-021-02873-0.
[6] J.-W. Heo, C.-H. Ho, T.-W. Park, W. Choi, J.-H. Jeong, and J. Kim, "Changes in cold surge occurrence over East Asia in the future: Role of thermal structure," *Atmosphere*, vol. 9, no. 6, p. 222, 2018. [Online]. Available: https://doi.org/10.3390/atmos9060222.
[7] Y. Zhang and C. Lu, "Detection of the synoptic southeastward-extending Siberian cold high during 1978–2017," *Atmospheric and Oceanic Science Letters*, vol. 15, p. 100140, 2022. [Online]. Available: https://doi.org/10.1016/j.aosl.2021.100140.
[8] A. Kumar, E. Y. M. Lo, and A. D. Switzer, "Relationship between East Asian Cold Surges and Synoptic Patterns: A New Coupling Framework," *Climate*, vol. 7, no. 2, p. 30, 2019. [Online]. Available: https://doi.org/10.3390/cli7020030.
[9] S. Y. Lim, C. Marzin, P. Xavier, C.-P. Chang, and B. Timbal, "Impacts of boreal winter monsoon cold surges and the interaction with MJO on Southeast Asia rainfall," *Journal of Climate*, vol. 30, no. 11, pp. 4267–4281, 2017. [Online]. Available: https://doi.org/10.1175/JCLI-D-16-0546.1
[10] M. R. Abdillah, Y. Kanno, T. Iwasaki, and J. Matsumoto, "Cold surge pathways in East Asia and their tropical impacts," *Journal of Climate*, vol. 34, no. 1, pp. 157-170, 2021. [Online]. Available: https://doi.org/10.1175/JCLI-D-20-0552.1.
[11] E. Saufina, R. Trismidianto, F. Risyanto, I. Fathrio, and W. Harjupa, "Impact of cross equatorial northerly surge (CENS) on Jakarta heavy rainfall and its interaction with tropical cyclone (Case study: 18–25 February 2020)," *AIP Conference Proceedings*, vol. 2366, p. 050002, 2021. [Online]. Available: https://doi.org/10.1063/5.0059995.
[12] M. Hattori, S. Mori, and J. Matsumoto, "The cross-equatorial northerly surge over the Maritime Continent and its relationship to precipitation patterns," *Journal of the Meteorological Society of Japan Ser. II*, vol. 89A, pp. 27-47, 2011. [Online]. Available: https://doi.org/10.2151/jmsj.2011-A02.
[13] R. R. Fauzi and R. Hidayat, "Role of cold surge and MJO on rainfall enhancement over Indonesia during East Asian winter monsoon," *IOP Conference Series: Earth and Environmental Science*, vol. 149, pp. 012045, 2018. [Online]. Available: https://doi.org/10.1088/1755-1315/149/1/012045.
[14] Q. Liu, L. Huang, and L. Bai, "Delayed effects of large-scale cold surge on winter heavy rainfall in southern China," *Atmospheric Research*, vol. 285, p. 106632, 2023. [Online]. Available: https://doi.org/10.1016/j.atmosres.2023.106632.
[15] P. Xavier, S. Y. Lim, M. F. A. B. Abdullah, M. Bala, S. N. Chenoli, A. S. Handayani, C. Marzin, D. Permana, F. Tangang, K. D. Williams, and D. J. Yik, "Seasonal dependence of cold surges and their interaction with the Madden–Julian Oscillation over Southeast Asia," *Journal of Climate*, vol. 33, no. 6, pp. 2467–2482, 2020. [Online]. Available: https://doi.org/10.1175/JCLI-D-19-0048.1.
[16] T. A. Lestari, M. S. B. Athallah, and Y. D. Haryanto, "Identification of cross-equatorial northerly surge (CENS) relationship to very heavy rain events in Jakarta," *Bulletin of Applied Mathematics and Mathematics Education*, vol. 3, no. 1, pp. 45–54, 2021. [Online]. Available: https://dx.doi.org/10.12928/bamme.v3i1.7340.
[17] E. Yulihastin, T. W. Hadi, N. S. Ningsih, and M. R. Syahputra, "Early morning peaks in the diurnal cycle of precipitation over the northern coast of West Java and possible influencing factors," *Annals of Geophysics*, vol. 38, pp. 231–242, 2020. [Online]. Available: https://doi.org/10.5194/angeo-38-231-2020.
[18] X. Sun and R. Wu, "Contribution of Wind Speed and Sea-Air Humidity Difference to the Latent Heat Flux-SST Relationship," *Ocean-Land-Atmosphere Research*, vol. 2022, Article ID 9815103, Sep. 2022, doi: 10.34133/2022/9815103. [Online]. Available: https://orcid.org/0000-0003-4712-2251.
[19] G. J. Zhang and M. J. McPhaden, "The Relationship between Sea Surface

Temperature and Latent Heat Flux in the Equatorial Pacific," Journal of Climate, vol. 8, no. 3, pp. 589-605, Mar. 1995, doi: 10.1175/1520-0442(1995)008<0589>2.0.CO;2.

[20] B. P. Kumar, M. F. Cronin, S. Joseph, M. Ravichandran, and N. Sureshkumar, "Latent heat flux sensitivity to sea surface temperature: Regional perspectives," *Journal of Climate*, vol. 30, no. 1, pp. 129–143, 2017. [Online]. Available: https://doi.org/10.1175/JCLI-D-16-0285.1.

[21] A. Wirasatriya, D. N. Sugianto, M. Helmi, L. Maslukah, R. T. Widiyandono, V. E. Herawati, P. Subardjo, G. Handoyo, Haryadi, J. Marwoto, A. A. D. Suryoputro, W. Atmodjo, and H. Setiyono, "Heat flux aspects on the seasonal variability of sea surface temperature in the Java Sea," *Ecology, Environment & Conservation*, vol. 25, no. 1, pp. 434-442, 2019. [Online]. Available: https://doc-pak.undip.ac.id/id/eprint/13244.

[22] NOAA (National Oceanic and Atmospheric Administration), "Cold and warm episodes by season," 2019. [Online]. Available: https://origin.cpc.ncep.noaa.gov/products/analysis_monitoring/ensostuff/ONI_v5.php. [Accessed: 9-Aug-2024].

[23] W. Zhang, S. Li, F.-F. Jin, R. Xie, C. Liu, M. F. Stuecker, and A. Xue, "ENSO regime changes responsible for decadal phase relationship variations between ENSO sea surface temperature and warm water volume," *Geophysical Research Letters*, vol. 46, no. 13, pp. 7063-7856, 2019. [Online]. Available: https://doi.org/10.1029/2019GL082943.

[24] B. Trewin, "Seasonal climate summary for the southern hemisphere (spring 2018): positive Indian Ocean Dipole and Australia's driest September on record," *J. Southern Hemisphere Earth Syst. Sci.*, vol. 70, no. 1, pp. 373-392, Nov. 2020, doi: 10.1071/ES20007.

[25] T. Utari, A. Y. Baeda, and C. Paotonan, "Study of the Madden-Julian Oscillation (MJO) Scheme in South Sulawesi Province," *J. Riset & Teknol. Terapan Kemaritiman*, vol. 1, no. 2, pp. 34-41, Dec. 2022. [Online]. Available: doi: 10.25042/jrt2k.122022.05.

[26] R. A. Madden and P. Julian, "Detection of a 40±50 day oscillation in the zonal wind in the tropical Pacific," J Atmos Sci, vol. 28, pp. 702–708, 1971.

[27] E. Beliyana, N. S. Ningsih, S. R. Gunawan, and A. Tarya, "Characteristics of Marine Heatwaves in the Indonesian Waters during the PDO, ENSO, and IOD Phases and Their Relationships to Net Surface Heat Flux," *Atmosphere*, vol. 14, no. 6, p. 1035, 2023. [Online]. Available: https://doi.org/10.3390/atmos14061035.

[28] H. Tomita, K. Kutsuwada, M. Kubota, and T. Hihara, "Advances in the Estimation of Global Surface Net Heat Flux Based on Satellite Observation: J-OFURO3 V1.1," *Frontiers in Marine Science*, vol. 8, 2021, Art. no. 612361. [Online]. Available: https://doi.org/10.3389/fmars.2021.612361

[29] W. Ge, L. Han, and X. Tang, "Surface radiation characteristics of the Ali area, Northern Tibetan Plateau," *Environ. Res. Commun.*, vol. 3, no. 4, p. 041006, Apr. 2021, doi: 10.1088/2515-7620/abf0f3.

[30] M. Lauster, P. Remmen, M. Fuchs, J. Teichmann, R. Streblow, and D. Müller, "Modelling long-wave radiation heat exchange for thermal network building simulations at urban scale using Modelica," in *Proc. 10th Int. Modelica Conf.*, Lund, Sweden, 10–12 Mar. 2014.

[31] J. Zhang and J. Li, Eds., *Spatial Cognitive Engine Technology*, Chapter 11, "Spacecraft," Academic Press, 2023, pp. 129-162. ISBN 9780323951074. [Online]. Available: https://doi.org/10.1016/B978-0-323-95107-4.00004-4.

[32] K. V. Shende, V. S. Shirsat, M. R. Ramesh Kumar, and K. V. Kale, "Artificial Neural Network Model for Prediction of Latent Heat Flux over Bay of Bengal," *Int. J. Comput. Sci. Eng.*, vol. 7, no. 5, May 2019. [Online]. Available: https://doi.org/10.26438/ijcse/v7i5.901905.

[33] N. N. Purwadani, *"Variation of Cross-Equatorial Northerly Surge Formation Characteristics and Its Impact on Rainfall in The Western Maritime Continent,"* M.S. thesis, Institut Teknologi Bandung, 2023.

[34] Y.-C. Zhang and W. Rossow, "Estimating meridional energy transports by the atmospheric and oceanic general circulations using boundary flux data," *J. Climate*, vol. 10, pp. 2358-2373, 1997. doi: 10.1175/1520-0442(1997)010<2358>2.0.CO;2.

[35] X. Sun and R. Wu, "Contribution of Wind Speed and Sea-Air Humidity Difference to the Latent Heat Flux-SST Relationship," *Ocean-Land-Atmosphere Research*, vol. 2022, Article ID: 9815103, Sep. 2022. doi: 10.34133/2022/9815103.
[36] H. Tomita and M. Kubota, "Variability of surface heat flux over the Indian Ocean" *Atmosphere-Ocean*, vol. 42, no. 3, pp. 183-199, 2004. doi: 10.3137/ao.420303.
[37] B.-X. Feng, H.-L. Liu, P.-F. Lin, and Q. Wang, "Estimation of the surface heat budget over the South China Sea," *Atmospheric and Oceanic Science Letters*, vol. 9, no. 3, pp. 191-197, 2016, doi: 10.1080/16742834.2016.1164011.